

Lack of pendrin HCO_3^- transport elevates vestibular endolymphatic $[\text{Ca}^{2+}]$ by inhibition of acid-sensitive TRPV5 and TRPV6 channels

Kazuhiro Nakaya,^{1,4} Donald G. Harbidge,¹ Philine Wangemann,²
Bruce D. Schultz,³ Eric D. Green,⁵ Susan M. Wall,⁶ and Daniel C. Marcus¹

¹Cellular Biophysics Laboratory, ²Cell Physiology Laboratory, and ³Epithelial Cell Biology Laboratory, Department of Anatomy and Physiology, Kansas State University, Manhattan, Kansas; ⁴Department of Otolaryngology-Head and Neck Surgery, Tohoku University Graduate School of Medicine, Sendai, Japan; ⁵Genome Technology Branch, National Human Genome Research Institute, National Institutes of Health, Bethesda, Maryland; and ⁶Renal Division, Emory University School of Medicine, Atlanta, Georgia

Submitted 30 October 2006; accepted in final form 29 December 2006

Nakaya K, Harbidge DG, Wangemann P, Schultz BD, Green ED, Wall SM, Marcus DC. Lack of pendrin HCO_3^- transport elevates vestibular endolymphatic $[\text{Ca}^{2+}]$ by inhibition of acid-sensitive TRPV5 and TRPV6 channels. *Am J Physiol Renal Physiol* 292: F1314–F1321, 2007. First published January 2, 2007; doi:10.1152/ajprenal.00432.2006.—The low Ca^{2+} concentration ($[\text{Ca}^{2+}]$) of mammalian endolymph in the inner ear is required for normal hearing and balance. We reported (Yamauchi et al., *Biochem Biophys Res Commun* 331: 1353–1357, 2005) that the epithelial Ca^{2+} channels TRPV5 and TRPV6 (transient receptor potential types 5 and 6) are expressed in the vestibular system and that TRPV5 expression is stimulated by 1,25-dihydroxyvitamin D_3 , as also reported in kidney. TRPV5/6 channels are known to be inhibited by extracellular acidic pH. Endolymphatic pH, $[\text{Ca}^{2+}]$, and transepithelial potential of the utricle were measured in $\text{Cl}^-/\text{HCO}_3^-$ exchanger pendrin (*SLC26A4*) knockout mice in vivo. *Slc26a4*^{-/-} mice exhibit reduced pH and utricular endolymphatic potential and increased $[\text{Ca}^{2+}]$. Monolayers of primary cultures of rat semicircular canal duct cells were grown on permeable supports, and cellular uptake of ⁴⁵ Ca^{2+} was measured individually from the apical and basolateral sides. Net uptake of ⁴⁵ Ca^{2+} was greater after incubation with 1,25-dihydroxyvitamin D_3 . Net ⁴⁵ Ca^{2+} absorption was dramatically inhibited by low apical pH and was stimulated by apical alkaline pH. Gadolinium, lanthanum, and ruthenium red reduced apical uptake. These observations support the notion that one aspect of vestibular dysfunction in Pendred syndrome is a pathological elevation of endolymphatic $[\text{Ca}^{2+}]$ due to luminal acidification and consequent inhibition of TRPV5/6-mediated Ca^{2+} absorption.

epithelial calcium channel; vitamin D; *SLC26a4*; HCO_3^- secretion

PENDRIN (PDS or *SLC26A4*) is an anion exchanger that is capable of transporting iodide, chloride, formate, nitrate, and bicarbonate and functions as an HCO_3^- -secreting mechanism in kidney (30, 31, 33). *SLC26A4* is expressed in kidney (29), the inner ear, thyroid (7), mammary gland (26), uterus (34), testis (16), vas deferens (3), and placenta (2). Mutation or deletion of the *SLC26A4* gene leads to acidification of the urine (15) and to Pendred syndrome, which is an autosomal recessive disorder characterized by sensorineural hearing loss and goiter (21, 25).

The availability of *SLC26A4* knockout mice (*Slc26a4*^{-/-}) makes it possible to perform a direct study of the inner ear defects that occur in the absence of *SLC26A4* (6). *Slc26a4*^{-/-} mice are completely deaf and also display signs of vestibular

dysfunction (6). In the vestibular system, pendrin is expressed in the apical membrane of vestibular transitional cells in the utricle and ampullae (40). If *SLC26A4* secretes HCO_3^- in the vestibule and if there are no strong compensatory mechanisms, it can be predicted that there may be an acidification of endolymph when *SLC26A4* is deleted. An altered endolymphatic pH can be expected to affect other ion transport processes in the luminal membrane of epithelial cells bordering the lumen, since several ion channels are known to be highly sensitive to extracellular pH.

The Ca^{2+} concentration ($[\text{Ca}^{2+}]$) of vestibular endolymph (~250 μM) is lower than that of perilymph (~1 mM), and it has a critical role in sensory transduction through hair cells (20). A Ca^{2+} absorption system in inner ear epithelial cells must be present to maintain the low $[\text{Ca}^{2+}]$ of vestibular endolymph. Recently, our group reported that the epithelial Ca^{2+} channels TRPV5 and TRPV6 (transient receptor potential types 5 and 6) are expressed in the semicircular canal duct (SCCD) of the vestibular system and that expression of TRPV5 is regulated by 1,25-dihydroxyvitamin D_3 [$1,25(\text{OH})_2\text{D}_3$], as in some other systems (9, 36, 44). TRPV5 and TRPV6 belong to the transient receptor potential (TRP) family of channels and are the only two highly Ca^{2+} -selective TRP channels (12, 22). TRPV5 is expressed in specific tissues such as kidney, placenta, and bone and plays a major role in Ca^{2+} transport and is localized at the apical membrane of epithelial cells or at the ruffled border membrane of osteoclasts (10, 11, 37). Recently, the molecular mechanisms of TRPV5/6 inhibition by both intra- and extracellular acidic pH were reported (45).

Because of the presence of the TRPV5/6 Ca^{2+} -absorptive pathway in the vestibular system and its known inhibition by extracellular acid in other systems, we hypothesized that part of the vestibular dysfunction observed in Pendred syndrome may be due to an acidification of endolymph (loss of HCO_3^- secretion), which in turn would lead to an elevation of luminal $[\text{Ca}^{2+}]$. We therefore sought to measure the luminal pH and $[\text{Ca}^{2+}]$ in wild-type (*Slc26a4*^{+/+}), heterozygous (*Slc26a4*^{+/-}), and knockout (*Slc26a4*^{-/-}) mice and to determine whether Ca^{2+} uptake across the apical and basolateral membranes of vestibular Ca^{2+} -absorbing epithelia was sensitive to apical acidification and to known TRPV5/6 blockers.

Address for reprint requests and other correspondence: D. C. Marcus, Kansas State Univ., Dept. of Anatomy and Physiology, 228 Coles Hall, Manhattan, KS 66506-5802 (e-mail: marcus@ksu.edu).

The costs of publication of this article were defrayed in part by the payment of page charges. The article must therefore be hereby marked "advertisement" in accordance with 18 U.S.C. Section 1734 solely to indicate this fact.

We indeed observed a reduced pH and increased $[Ca^{2+}]$ in the vestibular lumen of *Slc26a4*^{-/-} mice. Furthermore, 1,25(OH)₂D₃ increased ⁴⁵Ca²⁺ absorption and TRPV5/6 inhibitors reduced apical uptake of ⁴⁵Ca²⁺. ⁴⁵Ca²⁺ absorption was inhibited by apical acid pH and was stimulated by apical alkaline pH, consistent with the notion that one aspect of vestibular dysfunction in Pendred syndrome is a pathological elevation of endolymphatic $[Ca^{2+}]$ due to luminal acidification and consequent inhibition of TRPV5/6-mediated Ca²⁺ absorption.

METHODS

Utricular endolymphatic potential, pH, and $[Ca^{2+}]$. Adult *Slc26a4*^{-/-} and *Slc26a4*^{+/-} mice were obtained from a colony at Kansas State University that was established with breeders kindly provided by Dr. Susan Wall. The mouse strain 129Sv/Ev (Taconic, Germantown, NY) was used as the source of *Slc26a4*^{+/+} mice, since *Slc26a4*^{-/-} mice were generated in this background. Young adult mice 30–142 days old were deeply anesthetized with tribromoethanol (640 mg/kg ip; Fluka 90710) in 0.9% NaCl. The Institutional Animal Care and Use Committee of Kansas State University approved all experimental protocols.

We measured utricular endolymphatic potential (UP), pH, and $[Ca^{2+}]$ with double-barreled microelectrodes (one side pH or Ca²⁺ sensitive and the other voltage sensitive; see below for details) using procedures developed by modifying previously described protocols (18, 19). For both pH and Ca²⁺ electrodes, two pieces of glass tubing containing a glass filament (World Precision Instruments 1B100F-4, Sarasota, FL) were cut to 81 mm and 60 mm and pulled with a micropipette puller (Narishige PD-5, Tokyo, Japan). After pulled capillaries were heated at 180°C for 2 h, the ion-selective barrel was silanized by placing the open end of that barrel through a hole in the lid of a beaker at 210°C in which we put 0.08 ml of dimethyldichlorosilane (Fluka 40136) for 90 s. The reference barrel was protected from silanization by sealing the open end with Parafilm (Alcan Packaging). After electrodes were heated at 180°C for 3 h, the tips were broken to ~3 μm outer diameter.

For pH electrodes, the reference barrel was filled with 1 M KCl, and the ion-selective barrel was filled at the tip with hydrogen ionophore II-cocktail A (Fluka 95297) and back filled with buffer solution (500 mM KCl, 20 mM HEPES, pH 7.34). For Ca²⁺ electrodes, the reference barrel was filled with 150 mM KCl, and the ion-selective barrel was filled at the tip with calcium ionophore I-cocktail A (Fluka 21048) and back filled with 500 mM CaCl₂. Connection to each barrel was made with a Ag-AgCl wire. Each electrode was connected to an input of a dual electrometer (World Precision Instruments FD223), and buffered outputs were led to a data acquisition system (Axon Instruments DIGIDATA 1322A) and recorded with AxoScope 9 (Axon Instruments). A pulse generator was used to inject current pulses (1 nA) through the reference barrel to monitor the resistance of the electrode.

pH electrodes were calibrated at three different pH values (composition in mM): pH 6 (130 NaCl, 20 MES), pH 7 (130 NaCl, 20 HEPES), and pH 8 (130 NaCl, 20 tricine) and had an average slope of 56.6 ± 0.7 mV/pH (*n* = 16). Ca²⁺ electrodes were calibrated at three Ca²⁺ concentrations (composition in mM): 10 μM Ca²⁺ [0.121 CaCl₂, 150 KCl, 10 HEPES, 1 C₆H₇NO₆Na₂, (nitrilotriacetic acid; Sigma N-0128), pH 7.4], 100 μM Ca²⁺ (0.1 CaCl₂, 150 KCl, 10 HEPES, pH 7.4), and 1 mM Ca²⁺ (1 CaCl₂, 150 KCl, 10 HEPES, pH 7.4) and had an average slope of 26.2 ± 0.8 mV/decade concentration (*n* = 13). Data were analyzed with custom software written by P. Wangemann in LabTalk (Origin 6.0; OriginLab, Northampton, MA).

To reduce the diffusion of CO₂ through the exposed surface of the perilymph to the ambient air, which leads to higher pH than in unexposed perilymph, we put liquid Sylgard 184 (Dow Corning,

Midland, MI) at the fluid surface after placing the electrodes in the perilymph. The electrode was maintained below the surface of the perilymph solution after measurements were made of inner ear fluids, and the first calibration point was taken in situ in the bulla pocket of the temporal bone. The pH 7 buffer for calibration was placed on the Sylgard layer, and the electrode was retracted up into this buffer from the perilymph surrounding the utricle. Approximately 85% of the electrodes survived the travel through the Sylgard layer; outcomes from experiments in which electrodes failed this maneuver were excluded from the data set. The remaining calibration points to determine slope sensitivity were obtained by placing calibration solutions in a small-conducting Ringer-agarose (BP164; Fisher Scientific) cup that rested on the exposed neck muscles. This procedure was used to preclude voltage offsets introduced through movement of the reference electrode. In some cases, the electrode failed after moving to the calibration cup. In these few cases, the preexperiment electrode slope was used in conjunction with the in situ calibration point. Calibration of Ca²⁺ electrodes was identical except that the first point was taken by flushing the perilymph space with 1 mM Ca²⁺ solution and raising the electrode into a region of the pool remote from the tissues.

Perilymph pH, $[Ca^{2+}]$, and UP were corrected for the liquid junction potentials of 1.3 mV (pH electrode) and 4 mV (Ca²⁺ electrode) between the voltage barrels in calibrating solution and in perilymph and between the voltage electrode in perilymph and endolymph.

Cellular uptake measurements. Primary cultures of Wistar rat SCCD were prepared and incubated in DMEM-F-12 (12500-062; Invitrogen) supplemented with 5% fetal bovine serum, penicillin (100 U/ml), and streptomycin (100 μg/ml), as described previously (44). Primary cultures of SCCD cells from rats were used to study transport function because attempts to proliferate murine SCCD cells in culture were unsuccessful. Briefly, SCCD epithelial cells from neonatal rats were cultured on 12-mm-diameter Snapwell permeable supports (0.4-μm pore size, Costar 3801, Corning, NY). Confluence of primary cultures (10–14 days after seeding) was verified visually and by measurement of transepithelial electrical resistance using an Endohm meter (World Precision Instruments). Cultures were incubated further for 24 h in the presence or absence of 1,25(OH)₂D₃ (DM-200; Biomol, Plymouth Meeting, PA) (44).

The method for cellular ⁴⁵Ca²⁺ uptake determination was modified from Den Dekker et al. (5). Cells were washed twice on both sides with prewarmed Ca²⁺-free solution (in mM: 145 NaCl, 4 KCl, 1 MgCl₂, 20 HEPES, 5 glucose, pH 7.4). Cells were then incubated in this medium at 37°C and 5% CO₂ for 45–60 min before treatment. Cells tested with Ca²⁺ channel blockers or different pH buffers had the apical medium changed after 45 min of pretreatment, allowing 15-min incubation with the appropriate blocker or pH. The blocker medium was Ca²⁺-free solution with an added mixture of known inhibitors of TRPV5/6 (10 μM ruthenium red, 100 μM LaCl₃, and 100 μM GdCl₃) or each blocker in the same concentration by itself. The various pH buffers were similar to Ca²⁺-free solution except that the pH 5.5 contained 20 mM MES as a buffer in place of HEPES and the pH of each was adjusted with HCl or NaOH as appropriate. The pretreatment buffer on either the apical or basolateral side was replaced with ⁴⁵Ca²⁺ uptake buffer (in mM: 145 NaCl, 4 KCl, 1 MgCl₂, 0.1 CaCl₂, 20 HEPES, 5 glucose with 10 μM verapamil, pH 7.4, and at least 1 μCi ⁴⁵Ca²⁺/ml) for 15 min. Verapamil was utilized to preclude measuring Ca²⁺ uptake via L-type Ca²⁺ channels, which play important roles in some epithelia (27). Verapamil at the concentration used here is sufficient for a virtually complete block of Ca²⁺ current through these channels (13). The radiotracer was purchased as 1 mCi (37 MBq) ⁴⁵Ca²⁺ as CaCl₂ in 17 μl of H₂O (NEZ013001MC; Perkin-Elmer Life Sciences, Boston, MA).

The cells were then rinsed three times on both sides with ice-cold wash buffer (in mM: 145 NaCl, 4 KCl, 1 MgCl₂, 0.5 CaCl₂, 1.5 LaCl₃,

20 HEPES, 5 glucose, pH 7.4). The wash buffer was removed from both compartments, and 200 μ l of lysis buffer (lysis reagent 1 from cAMP kit RPN225; Amersham Biosciences, Piscataway, NJ) were added to the apical compartment. After 5 min, the lysate was collected and radioactivity was determined with a liquid scintillation counter (Packard Tri-Carb 2100TR, Meriden, CT). The difference in uptake of $^{45}Ca^{2+}$ from the apical and basolateral sides was taken as a relative measure of net flux.

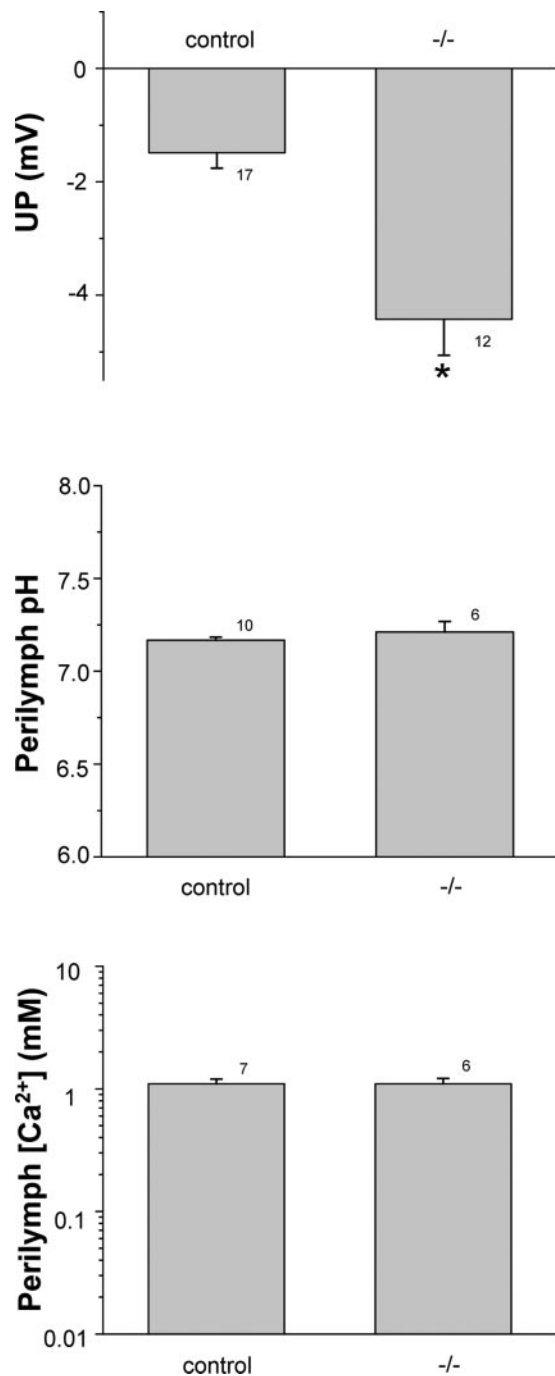


Fig. 1. Utricular endolymphatic potential (UP), perilymphatic pH, and Ca^{2+} concentration ($[Ca^{2+}]$). *Top*: UP of pooled (control) wild-type ($Slc26a4^{+/+}$; $n = 8$) and heterozygous ($Slc26a4^{+/-}$; $n = 9$) mice and of knockout ($Slc26a4^{-/-}$) mice. * $P < 0.05$. *Middle*: perilymphatic pH of control and knockout mice. No significant difference is shown ($P > 0.05$). *Bottom*: perilymphatic $[Ca^{2+}]$ of control and knockout mice. No significant difference ($P > 0.05$) is shown. Numbers of measurements are indicated at each bar.

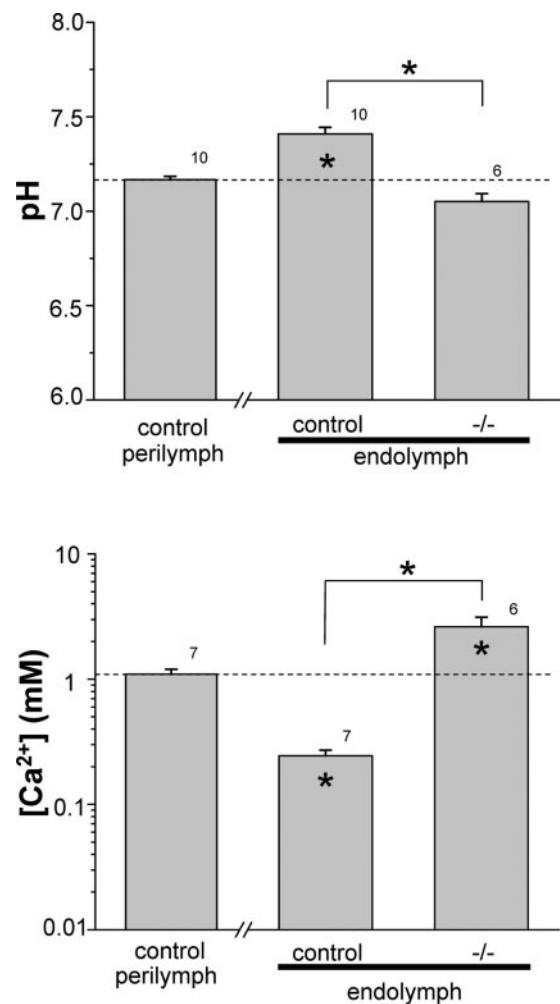


Fig. 2. Endolymphatic pH and $[Ca^{2+}]$. *Top*: endolymphatic pH of control and knockout ($-/-$) genotypes compared with control perilymphatic pH (dotted line). *Bottom*: endolymphatic $[Ca^{2+}]$ of control and knockout ($-/-$) genotypes compared with control perilymphatic pH (dotted line). Numbers of measurements are indicated at each bar. *Inside bars: $P < 0.05$ vs. perilymphatic pH or $[Ca^{2+}]$. *Above brackets: $P < 0.05$.

Statistics. Data are presented as means \pm SE from n observations. Net uptakes are the difference of the mean apical and basolateral uptakes; the SE was pooled from the variance of the apical and basolateral uptake data, as calculated from the variances with the Java applet at <http://home.ubalt.edu/ntsbarsh/Business-stat/otherapplets/Pooled.htm>. Significance between the UP, pH, and Ca^{2+} control and knockout mouse data and the significance of Ca^{2+} uptake data were calculated with an unpaired t -test. Comparison of endolymph values to the corresponding perilymph values (see Fig. 2) was performed with paired t -test. $P < 0.05$ represents a significant difference.

RESULTS

UP, pH, and $[Ca^{2+}]$ in the utricle. Across all measurements, $Slc26a4^{+/-}$ mice showed no significant differences in UP, pH, and $[Ca^{2+}]$ compared with $Slc26a4^{+/+}$ mice, consistent with an autosomal recessive trait. There were no differences between $Slc26a4^{+/+}$ mice compared with $Slc26a4^{+/-}$ mice in UP [-1.5 ± 0.5 mV ($n = 8$) vs. -1.5 ± 0.3 mV ($n = 9$)], perilymphatic pH [7.14 ± 0.02 ($n = 5$) vs. 7.19 ± 0.02 ($n = 5$)], endolymphatic pH [7.42 ± 0.02 ($n = 5$) vs. 7.40 ± 0.06

($n = 5$), perilymphatic $[Ca^{2+}]$ [1.62 ± 0.10 mM ($n = 3$) vs. 1.51 ± 0.28 mM ($n = 4$)], endolymphatic $[Ca^{2+}]$ [266 ± 51 μ M ($n = 3$) vs. 230 ± 28 μ M ($n = 4$)]. The data and the SE were pooled between the two genotypes and taken as "control" reference values against which the knockout mice were evaluated.

There was a small, but statistically significant, decrease of ~ 3 mV in the UP of *Slc26a4*^{-/-} mice compared with control mice (Fig. 1). No significant differences between the control and knockout mice were observed in perilymphatic pH and $[Ca^{2+}]$ (Fig. 1). The pH was higher in endolymph of control mice than in the perilymph, consistent with secretion of HCO_3^- by pendrin. Endolymphatic pH was significantly decreased in *Slc26a4*^{-/-} mice compared with control mice (Fig. 2). Furthermore, endolymphatic $[Ca^{2+}]$ was less than in perilymph of control mice and was significantly increased in *Slc26a4*^{-/-} mice to a level higher than in perilymph (Fig. 2). These abnormalities of endolymphatic potential, pH, and $[Ca^{2+}]$ in *Slc26a4*^{-/-} mice are compatible with their vestibular dysfunction, exhibited as circling behavior and head tilting (6).

The high endolymphatic $[Ca^{2+}]$ in *Slc26a4*^{-/-} mice would be consistent with altered otoconia, as reported earlier (41). Indeed, we consistently observed an absence of the normal otoconia but observed a single giant crystal (Fig. 3), assumed to be $CaCO_3$, which is the compound of calcium observed in otoconia.

Increased Ca^{2+} absorption by $1,25(OH)_2D_3$. We tested whether Ca^{2+} absorption is stimulated by exposure to $1,25(OH)_2D_3$,

since transcript expression of two genes involved in epithelial Ca^{2+} absorption, TRPV5 and calbindin, is upregulated (44). Stimulation of transport would therefore serve as part of the fingerprint for the involvement of this Ca^{2+} transport system in vestibular function.

Apical-to-cell $^{45}Ca^{2+}$ uptake and basolateral-to-cell $^{45}Ca^{2+}$ uptake in primary SCCD cells were measured separately. Net uptake was obtained by subtraction of the mean basolateral-to-cell $^{45}Ca^{2+}$ uptake from the mean apical-to-cell $^{45}Ca^{2+}$ uptake. Without any added inhibitors of TRPV5/6, cultured cells exhibited a net $^{45}Ca^{2+}$ uptake consistent with an absorptive flux from the apical to the basolateral side (Fig. 4). This direction corresponds to endolymph (normally, low $[Ca^{2+}]$) to perilymph (normally, high $[Ca^{2+}]$). Incubation with $1,25(OH)_2D_3$ for 24 h significantly increased net Ca^{2+} uptake by 71% (Fig. 4).

Regulation by pH. The pH of the apical solution was varied over a wide range to test the dependence of Ca^{2+} uptake on apical pH of the SCCD cells. Decreases of the apical pH from 8.2 to 7.4 and 5.5 each significantly reduced net $^{45}Ca^{2+}$ uptake by 37 and 96%, respectively (Fig. 5).

Inhibition of Ca^{2+} uptake by inhibitors. Adding a mixture of agents known to block TRPV5 and TRPV6 Ca^{2+} channels (in μ M: 10 ruthenium red, 100 $LaCl_3$, 100 $GdCl_3$) stopped the net uptake completely (Fig. 6A). Both apical-to-cell and basolateral-to-cell uptakes were significantly reduced (Fig. 6A). Because the mixture of Ca^{2+} inhibitors completely blocked Ca^{2+} net uptake, individual blockers were examined.

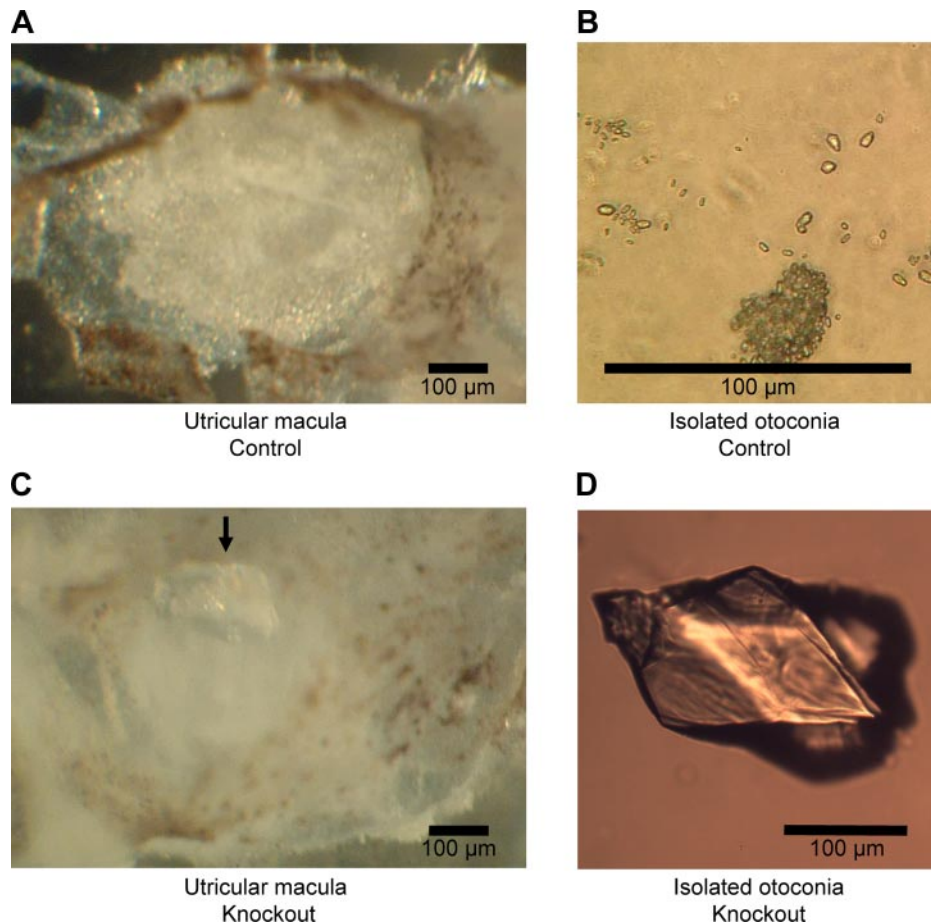
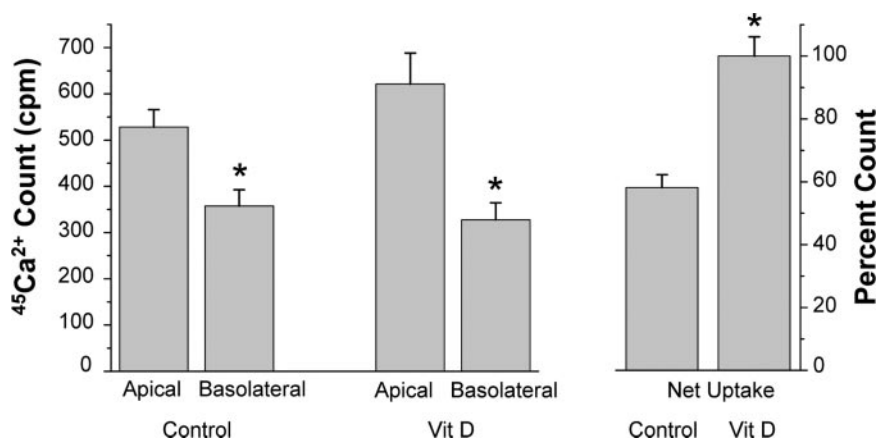


Fig. 3. Otoconia from control (*Slc26a4*^{+/-}) and knockout (*Slc26a4*^{-/-}) mice. A: normal otoconia situated in utricle from *Slc26a4*^{+/-} mouse. B: normal otoconia isolated from *Slc26a4*^{+/-} utricle at higher magnification. C: utricle from *Slc26a4*^{-/-} mouse with giant crystal (arrow). D: giant crystal isolated from *Slc26a4*^{-/-} utricle at higher magnification.

Fig. 4. Upregulation of $^{45}Ca^{2+}$ uptake by 1,25-dihydroxyvitamin D_3 [$1,25(OH)_2D_3$] across semicircular canal duct (SCCD) cells grown on permeable supports. *Left*: apical-to-cell $^{45}Ca^{2+}$ uptake (apical) and basolateral-to-cell $^{45}Ca^{2+}$ uptake (basolateral) of cells incubated with and without 1,25(OH) $_2D_3$ (Vit D, 100 nM, 24 h). *Right*: net $^{45}Ca^{2+}$ uptake was calculated by subtracting mean basolateral-to-cell $^{45}Ca^{2+}$ uptake from mean apical-to-basolateral $^{45}Ca^{2+}$ uptake; SE values were pooled. Net $^{45}Ca^{2+}$ uptake of cells with 1,25(OH) $_2D_3$ was regarded as 100% ($n = 4$). Uptakes are expressed as counts per minute (cpm). * $P < 0.05$.



Ruthenium red (10 μM) significantly decreased net Ca^{2+} uptake by 31% (Fig. 6B); 100 μM $LaCl_3$ and 100 μM $GdCl_3$ showed stronger effects than ruthenium red (Fig. 6C).

DISCUSSION

We report for the first time that *Slc26a4* $^{-/-}$ mice possess a markedly lower pH and higher $[Ca^{2+}]$ in the luminal fluid, endolymph, than wild-type and heterozygous mice. We also present the first evidence of net Ca^{2+} absorption by SCCD epithelium in the vestibular system.

SLC26A4 is expressed in several discrete areas in the inner ear, including the apical membrane of vestibular transitional cells of the utricle and ampullae of the semicircular canals (8, 40). These observations, along with the absence of pendrin transcript in the SCCD (N. Raveendran and D. Marcus, unpublished observations), suggest that pH homeostatic contributions by the Cl^-/HCO_3^- exchanger pendrin occurs mainly outside of the SCCD.

Despite the physical separation between the sites of HCO_3^- secretion and of calcium absorption, it is expected that there is no significant gradient of pH among the utricle, ampullae, and canal ducts since the lumen has a relatively large cross-sectional area that favors good diffusion, unlike most smaller tubular epithelial structures such as the nephron. The volume

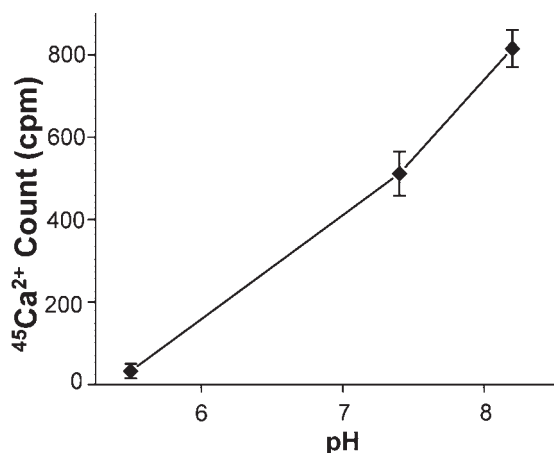


Fig. 5. Net $^{45}Ca^{2+}$ uptake under different apical pH levels. Measurements were made after a 15-min incubation with pH 5.5, 7.4, and 8.2. All cells were incubated with 1,25(OH) $_2D_3$ (100 nM, 24 h) before measurement ($n = 6$).

of the utricle is almost as large as the SCCD (32), and convection of endolymph through the SCCD is one of the mechanisms of vestibular perception (14, 39). It is thus reasonable to assume that both the utricle and the SCCD have similar ion concentrations and pH by diffusion and convection. The TRPV5/6 channels in the SCCD would therefore be exposed on their extracellular face to the relatively acidic conditions in the *Slc26a4* $^{-/-}$ mice.

Regulation of luminal pH by SLC26A4 could conceivably influence transport of a number of ions that are actively moved by vestibular epithelial cells. However, the deletion of SLC26A4 had no effect on luminal (endolymphatic) K^+ concentration in the utricle (28), suggesting that neither the K^+ secretory channel in the apical membrane of vestibular dark cells nor K^+ exit pathways are strongly sensitive to luminal pH. However, the negative shift of the UP in *Slc26a4* $^{-/-}$ mice is consistent with an increase in apical membrane conductance of highly polarized epithelial cells, such as the hair cells (17), as opposed to low-voltage K^+ -secretory dark cells (41). Increased apical conductance would increase the fractional contribution of the negative intracellular potential to the observed transepithelial potential, the UP (17). A candidate for the apical acid-activated conductance is the ASIC1b channel identified in the apical membrane of vestibular hair cells (35), although this channel in an oocyte expression system was only transiently activated by acid. ASIC1b inactivated during exposure to a step change in acid with a time constant on the order of 1 s (1).

Previously, we reported the expression of the epithelial Ca^{2+} channels TRPV5 and TRPV6 in primary cultures of SCCD epithelial cells (44). Because of the known sensitivity of the TRPV5 and TRPV6 channels to external pH (46), we hypothesized that low pH of vestibular endolymph due to absence of the Cl^-/HCO_3^- exchanger pendrin inhibits TRPV5 and TRPV6 and consequently leads to higher $[Ca^{2+}]$ in endolymph.

The normal $[Ca^{2+}]$ of vestibular endolymph ($\sim 250 \mu M$) (42) is known to be necessary for optimal hair cell function (20) and is likely important in the utricle for proper otoconial formation, which contains precipitated $CaCO_3$. The otoconial crystals comprise the inertial mass that is coupled to the sensory stereocilia of the utricular hair cells and are relatively fine "stones" under normal conditions but form giant crystals in *Slc26a4* $^{-/-}$ mice (Fig. 3) (40). The low $[Ca^{2+}]$ of normal endolymph points to the existence of one or more Ca^{2+} absorption pathways in the vestibular system. However, in

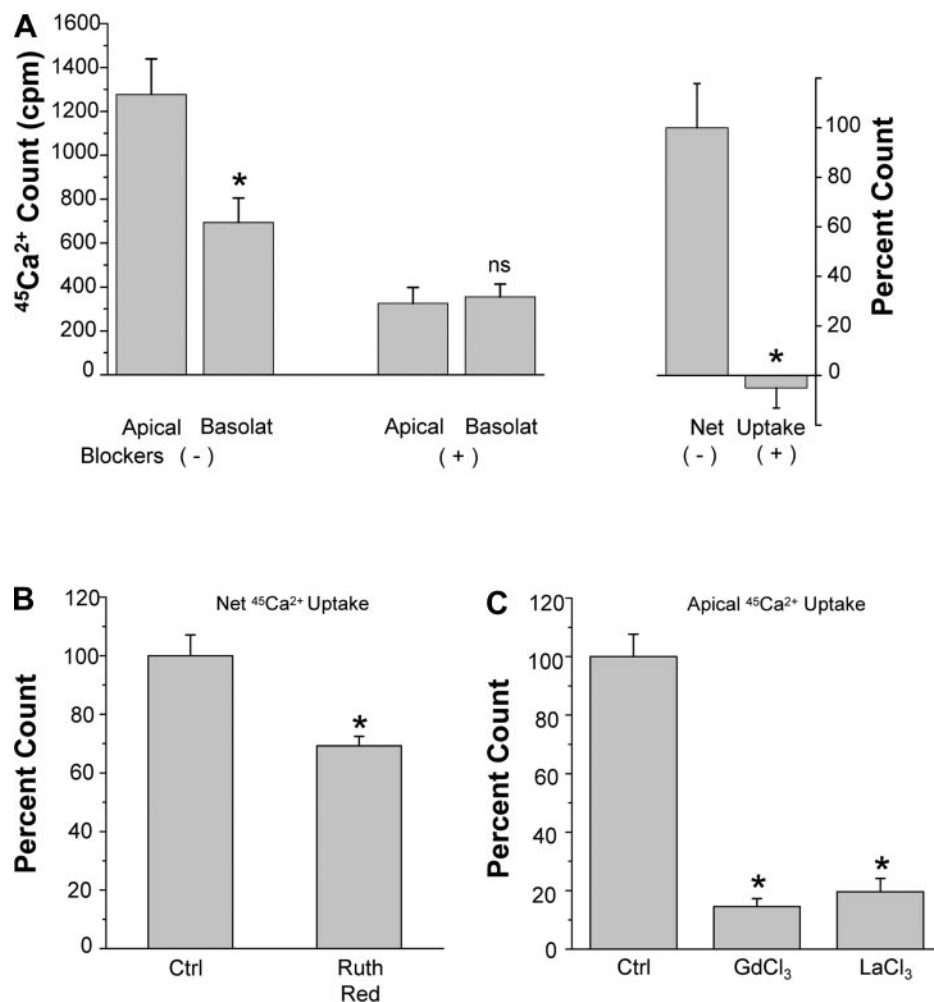


Fig. 6. Inhibition of $^{45}Ca^{2+}$ uptake into SCCD cells by TRPV5/6 inhibitors. SCCD cells were incubated with $1,25(OH)_2D_3$ (100 nM, 24 h) before the measurement. *A, left*: apical-to-cell $^{45}Ca^{2+}$ uptake (apical) and basolateral-to-cell $^{45}Ca^{2+}$ uptake (basolat) of cells with and without the mixture of Ca^{2+} inhibitors (in μM : 10 ruthenium red, 100 GdCl₃, 100 LaCl₃). *A, right*: net $^{45}Ca^{2+}$ uptake was calculated by subtracting mean basolateral-to-cell $^{45}Ca^{2+}$ uptake from mean apical-to-basolateral $^{45}Ca^{2+}$ uptake; SE values were pooled. Net $^{45}Ca^{2+}$ uptake of cells without the mixture of Ca^{2+} inhibitors was taken as 100% ($n = 6$). *B*: net $^{45}Ca^{2+}$ uptake of control and ruthenium red-treated cells ($n = 4$). $^{45}Ca^{2+}$ uptake of cells without inhibitor was taken as 100%. *C*: apical-to-cell $^{45}Ca^{2+}$ uptake of control, gadolinium-treated (GdCl₃), and lanthanum-treated (LaCl₃) cells ($n = 4$). $^{45}Ca^{2+}$ uptake of cells without inhibitor was taken as 100%. Concentrations for individual inhibitors are same as described in *A*. Ctrl, control; Ruth Red, ruthenium red. * $P < 0.05$. ns, Not significant.

addition to absorption, it is known that there are also Ca^{2+} secretory processes in the inner ear. The plasma membrane Ca^{2+} -ATPase isoform 2 is expressed in the apical membrane (stereocilia) of hair cells, and mutation of this isoform leads to an absence of otoconia, a lowered $[Ca^{2+}]$, and vestibular dysfunction (43).

Our results here of elevated $[Ca^{2+}]$ in the endolymph of *Slc26a4*^{-/-} mice compared with the endolymph of wild-type mice is consistent with inhibition of the Ca^{2+} -absorbing function of the TRPV5 and TRPV6 channels by acidic pH in those mice. Interestingly, endolymphatic $[Ca^{2+}]$ was also higher than the abluminal fluid, perilymph, in *Slc26a4*^{-/-} mice. That elevation of endolymphatic $[Ca^{2+}]$ (2.6 mM compared with 1.1 mM in perilymph) is even higher than the equilibrium concentration of 1.5 mM that could be accounted for by passive distribution of Ca^{2+} at the UP of -4.4 mV in knockout mice. These observations point to continued active secretion of Ca^{2+} in the vestibular system in the face of inhibited Ca^{2+} absorption.

TRPV5 is predominantly expressed and controlled by $1,25(OH)_2D_3$ in the kidney, whereas TRPV6 is predominantly expressed and controlled by $1,25(OH)_2D_3$ in the intestine (9, 36). Although the SCCD epithelium expresses transcripts for both TRPV5 and TRPV6, only TRPV5 is responsive to $1,25(OH)_2D_3$ in SCCD primary cultures (44) and expression of TRPV6 is ~ 10 -fold less in the native epithelium (D. Yamauchi,

N. Raveendran, D. Marcus; unpublished observations). Our observation of increased Ca^{2+} absorption by SCCD is consistent with observations in kidney and with the increased expression of TRPV5 transcript by $1,25(OH)_2D_3$ in SCCD.

Both intra- and extracellular acid pH inhibit TRPV5, and they each enhance the other's effect (45). Binding of extracellular protons to glutamate 522 in the pore region of TRPV5 causes conformational changes and closure of the channel (46). TRPV6 has a histidine at the position equivalent to glutamate 522 in TRPV5, which predicts similar pH sensitivity for both TRPV5 and TRPV6 (46). The very steep dependence of activity of these channels and of SCCD Ca^{2+} uptake on pH is strong evidence for the functional expression of the TRPV5 and TRPV6 channels in the apical membrane of SCCD epithelium.

In addition, TRPV5 is known to be inhibited by ruthenium red, gadolinium, and lanthanum (12, 38). TRPV6 is also inhibited by ruthenium red but with less potency [IC_{50} of 0.12 μM rabbit TRPV5 vs. 9 μM mouse TRPV6 (12)]. Each of the multivalent blockers has poor specificity, but the effectiveness of all of these conditions to decrease Ca^{2+} absorption in SCCD epithelium strongly supports the notion that a major part of the Ca^{2+} absorption from the semicircular canal is via the TRPV5 and TRPV6 channels. Ruthenium red is an inhibitor of a wide range of Ca^{2+} channels, including voltage-gated and epithelial

Ca^{2+} channels (4, 12). The net Ca^{2+} uptake in the SCCD was inhibited only 31% by 10 μ M ruthenium red despite the 100 \times lower IC_{50} mentioned above for TRPV5 and IC_{50} for TRPV6 similar to the concentration used. This result suggests either that there is a significant contribution of another Ca^{2+} -permeable channel in this epithelium or, more likely, points to a combination of species and condition differences to the cited studies.

The trivalent cations La^{3+} and Gd^{3+} are also effective blockers of TRPV5 and TRPV6 (23, 38) but are also not specific enough to discriminate TRPV5 and TRPV6 from other Ca^{2+} channels. In our study, a mixture of ruthenium red, La^{3+} , and Gd^{3+} produced a complete block of net Ca^{2+} uptake.

Vectorial Ca^{2+} absorption occurs by well-characterized processes (10). Ca^{2+} enters the cell from the lumen down an electrochemical gradient through TRPV5 and TRPV6 in the apical cell membrane. Cytotoxic accumulation of Ca^{2+} in the cytosol is prevented by immediate binding of Ca^{2+} to Ca^{2+} -binding proteins, calbindin-9K, and/or calbindin-28K, which carry Ca^{2+} in a bound state by diffusion to the basolateral cell membrane. Ca^{2+} is then extruded from the cell by an ATP-dependent plasma membrane Ca^{2+} -ATPase and an Na^+/Ca^{2+} exchanger. In this way, influx at the apical membrane and apical-to-basolateral flux are correlated in a 1:1 fashion (24). The radiotracer accumulation in the cells from the basolateral side predominantly indicates the basolateral-to-cell unidirectional cycle of the Na^+/Ca^{2+} exchanger. As the net flux is reduced, this coupled basolateral uptake will also be reduced, as seen in Fig. 6.

In conclusion, we have demonstrated an acid-sensitive vectorial Ca^{2+} absorption by the SCCD that can account for the pathological endolymph composition observed in mice with the SLC26A4 mutation. These observations increase our understanding of the etiology of Pendred syndrome.

ACKNOWLEDGMENTS

We thank Dr. Daisuke Yamauchi and Dr. Tao Wu for technical advice with endolymphatic pH and $[Ca^{2+}]$ measurements.

GRANTS

This work was supported by National Institutes of Health Grants R01 DC-00212 (D. C. Marcus), R01 DC-01098 (P. Wangemann), and PO1 DK-061521, project 2 (S. M. Wall) and US Department of Agriculture Grant 2003-35206-14157 (B. D. Schultz).

REFERENCES

- Bässler EL, Ngo-Anh TJ, Geisler HS, Ruppertsberg JP, Gründer S. Molecular and functional characterization of acid-sensing ion channel (ASIC) 1b. *J Biol Chem* 276: 33782–33787, 2001.
- Bidart JM, Lacroix L, Evain-Brion D, Caillou B, Lazar V, Frydman R, Bellet D, Filetti S, Schlumberger M. Expression of Na^+/I^- symporter and pendred syndrome genes in trophoblast cells. *J Clin Endocrinol Metab* 85: 4367–4372, 2000.
- Carlin RW, Sedlacek RL, Quesnell RR, Pierucci-Alves F, Grieger DM, Schultz BD. PVD9902, a porcine vas deferens epithelial cell line that exhibits neurotransmitter-stimulated anion secretion and expresses numerous HCO_3^- transporters. *Am J Physiol Cell Physiol* 290: C1560–C1571, 2006.
- Cibulsky SM, Sather WA. Block by ruthenium red of cloned neuronal voltage-gated calcium channels. *J Pharmacol Exp Ther* 289: 1447–1453, 1999.
- Den Dekker E, Schoeber J, Topala CN, Van de Graaf SF, Hoenderop JG, Bindels RJ. Characterization of a Madin-Darby canine kidney cell line stably expressing TRPV5. *Pflügers Arch* 450: 236–244, 2005.
- Everett LA, Belyantseva IA, Noben-Trauth K, Cantos R, Chen A, Thakkar SI, Hoogstraten-Miller SL, Kachar B, Wu DK, Green ED. Targeted disruption of mouse Pds provides insight about the inner-ear defects encountered in Pendred syndrome. *Hum Mol Genet* 10: 153–161, 2001.
- Everett LA, Glaser B, Beck JC, Idol JR, Buchs A, Heyman M, Adawi F, Hazani E, Nassir E, Baxevas AD, Sheffield VC, Green ED. Pendred syndrome is caused by mutations in a putative sulphate transporter gene (PDS). *Nat Genet* 17: 411–422, 1997.
- Everett LA, Morsli H, Wu DK, Green ED. Expression pattern of the mouse ortholog of the Pendred's syndrome gene (Pds) suggests a key role for pendrin in the inner ear. *Proc Natl Acad Sci USA* 96: 9727–9732, 1999.
- Hoenderop JG, Muller D, Van der Kemp AW, Hartog A, Suzuki M, Ishibashi K, Imai M, Sweep F, Willems PH, Van Os CH, Bindels RJ. Calcitriol controls the epithelial calcium channel in kidney. *J Am Soc Nephrol* 12: 1342–1349, 2001.
- Hoenderop JG, Nilius B, Bindels RJ. Calcium absorption across epithelia. *Physiol Rev* 85: 373–422, 2005.
- Hoenderop JG, Van der Kemp AW, Hartog A, Van de Graaf SF, Van Os CH, Willems PH, Bindels RJ. Molecular identification of the apical Ca^{2+} channel in 1, 25-dihydroxyvitamin D3-responsive epithelia. *J Biol Chem* 274: 8375–8378, 1999.
- Hoenderop JG, Vennekens R, Muller D, Prenen J, Droogmans G, Bindels RJ, Nilius B. Function and expression of the epithelial Ca^{2+} channel family: comparison of mammalian ECaC1 and 2. *J Physiol* 537: 747–761, 2001.
- Hu XD, Qian JQ. DDPH inhibited L-type calcium current and sodium current in single ventricular myocyte of guinea pig. *Acta Pharmacol Sin* 22: 415–419, 2001.
- Kassemi M, Oas JG, Deserranno D. Fluid-structural dynamics of ground-based and microgravity caloric tests. *J Vestib Res* 15: 93–107, 2005.
- Kim YH, Verlander JW, Matthews SW, Kurtz I, Shin W, Weiner ID, Everett LA, Green ED, Nielsen S, Wall SM. Intercalated cell H^+/OH^- transporter expression is reduced in Slc26a4 null mice. *Am J Physiol Renal Physiol* 289: F1262–F1272, 2005.
- Lacroix L, Mian C, Caillou B, Talbot M, Filetti S, Schlumberger M, Bidart JM. Na^+/I^- symporter and Pendred syndrome gene and protein expressions in human extra-thyroidal tissues. *Eur J Endocrinol* 144: 297–302, 2001.
- Marcus DC, Liu J, Wangemann P. Transepithelial voltage and resistance of vestibular dark cell epithelium from the gerbil ampulla. *Hear Res* 73: 101–108, 1994.
- Marcus DC, Wu T, Wangemann P, Kofuji P. KCNJ10 (Kir4.1) potassium channel knockout abolishes endocochlear potential. *Am J Physiol Cell Physiol* 282: C403–C407, 2002.
- Marcus NY, Marcus DC. Potassium secretion by nonsensory region of gerbil utricle in vitro. *Am J Physiol Renal Fluid Electrolyte Physiol* 253: F613–F621, 1987.
- Marquis RE, Hudspeth AJ. Effects of extracellular Ca^{2+} concentration on hair-bundle stiffness and gating-spring integrity in hair cells. *Proc Natl Acad Sci USA* 94: 11923–11928, 1997.
- Pendred V. Deaf-mutism and goitre. *Lancet* II: 532–535, 1896.
- Peng JB, Brown EM, Hediger MA. Apical entry channels in calcium-transporting epithelia. *News Physiol Sci* 18: 158–163, 2003.
- Peng JB, Chen XZ, Berger UV, Vassilev PM, Tsukaguchi H, Brown EM, Hediger MA. Molecular cloning and characterization of a channel-like transporter mediating intestinal calcium absorption. *J Biol Chem* 274: 22739–22746, 1999.
- Raber G, Willems PH, Lang F, Nitschke R, Van Os CH, Bindels RJ. Co-ordinated control of apical calcium influx and basolateral calcium efflux in rabbit cortical collecting system. *Cell Calcium* 22: 157–166, 1997.
- Reardon W, Coffey R, Phelps PD, Luxon LM, Stephens D, Kendall-Taylor P, Britton KE, Grossman A, Trembath R. Pendred syndrome—100 years of underascertainment? *QJM* 90: 443–447, 1997.
- Rillema JA, Hill MA. Prolactin regulation of the pendrin-iodide transporter in the mammary gland. *Am J Physiol Endocrinol Metab* 284: E25–E28, 2003.
- Rosenthal R, Strauss O. Ca^{2+} -channels in the RPE. *Adv Exp Med Biol* 514: 225–235, 2002.
- Royaux IE, Belyantseva IA, Wu T, Kachar B, Everett LA, Marcus DC, Green ED. Localization and functional studies of pendrin in the

- mouse inner ear provide insight about the etiology of deafness in pendred syndrome. *J Assoc Res Otolaryngol* 4: 394–404, 2003.
29. **Royaux IE, Wall SM, Karniski LP, Everett LA, Suzuki K, Knepper MA, Green ED.** Pendrin, encoded by the Pendred syndrome gene, resides in the apical region of renal intercalated cells and mediates bicarbonate secretion. *Proc Natl Acad Sci USA* 98: 4221–4226, 2001.
 30. **Scott DA, Karniski LP.** Human pendrin expressed in *Xenopus laevis* oocytes mediates chloride/formate exchange. *Am J Physiol Cell Physiol* 278: C207–C211, 2000.
 31. **Scott DA, Wang R, Kreman TM, Sheffield VC, Karniski LP.** The Pendred syndrome gene encodes a chloride-iodide transport protein. *Nat Genet* 21: 440–443, 1999.
 32. **Shinomori Y, Spack DS, Jones DD, Kimura RS.** Volumetric and dimensional analysis of the guinea pig inner ear. *Ann Otol Rhinol Laryngol* 110: 91–98, 2001.
 33. **Soleimani M, Greeley T, Petrovic S, Wang Z, Amlal H, Kopp P, Burnham CE.** Pendrin: an apical $Cl^{-}/OH^{-}/HCO_3^{-}$ exchanger in the kidney cortex. *Am J Physiol Renal Physiol* 280: F356–F364, 2001.
 34. **Suzuki K, Royaux IE, Everett LA, Mori-Aoki A, Suzuki S, Nakamura K, Sakai T, Katoh R, Toda S, Green ED, Kohn LD.** Expression of PDS/Pds, the Pendred syndrome gene, in endometrium. *J Clin Endocrinol Metab* 87: 938, 2002.
 35. **Ugawa S, Inagaki A, Yamamura H, Ueda T, Ishida Y, Kajita K, Shimizu H, Shimada S.** Acid-sensing ion channel-1b in the stereocilia of mammalian cochlear hair cells. *Neuroreport* 17: 1235–1239, 2006.
 36. **Van Cromphaut SJ, Dewerchin M, Hoenderop JG, Stockmans I, Van Herck E, Kato S, Bindels RJ, Collen D, Carmeliet P, Bouillon R, Carmeliet G.** Duodenal calcium absorption in vitamin D receptor-knock-out mice: functional and molecular aspects. *Proc Natl Acad Sci USA* 98: 13324–13329, 2001.
 37. **Van der Eerden BC, Hoenderop JG, de Vries TJ, Schoenmaker T, Buurman CJ, Uitterlinden AG, Pols HA, Bindels RJ, van Leeuwen JP.** The epithelial Ca^{2+} channel TRPV5 is essential for proper osteoclastic bone resorption. *Proc Natl Acad Sci USA* 102: 17507–17512, 2005.
 38. **Vennekens R, Prenen J, Hoenderop JG, Bindels RJ, Droogmans G, Nilius B.** Pore properties and ionic block of the rabbit epithelial calcium channel expressed in HEK 293 cells. *J Physiol* 530: 183–191, 2001.
 39. **Wada Y, Suzuki H, Watanabe S.** Changes of ampulla pressure in the semicircular canal of pigeons by caloric stimulation. *Acta Astronaut* 33: 15–18, 1994.
 40. **Wangemann P, Itza EM, Albrecht B, Wu T, Jabba SV, Maganti RJ, Lee JH, Everett LA, Wall SM, Royaux IE, Green ED, Marcus DC.** Loss of KCNJ10 protein expression abolishes endocochlear potential and causes deafness in Pendred syndrome mouse model. *BMC Med* 2: 30, 2004.
 41. **Wangemann P, Marcus DC.** The membrane potential of vestibular dark cells is controlled by a large Cl^{-} conductance. *Hear Res* 62: 149–156, 1992.
 42. **Wangemann P, Schacht J.** Homeostatic mechanisms in the cochlea. In: *The Cochlea*, edited by Dallos P, Popper AN and Fay RR. New York: Springer-Verlag, 1996, p. 130–185.
 43. **Wood JD, Muchinsky SJ, Filoteo AG, Penniston JT, Tempel BL.** Low endolymph calcium concentrations in deafwaddler2J mice suggest that PMCA2 contributes to endolymph calcium maintenance. *J Assoc Res Otolaryngol* 5: 99–110, 2004.
 44. **Yamauchi D, Raveendran NN, Pondugula SR, Kampalli SB, Sanneman JD, Harbidge DG, Marcus DC.** Vitamin D upregulates expression of ECAC1 mRNA in semicircular canal. *Biochem Biophys Res Commun* 331: 1353–1357, 2005.
 45. **Yeh BI, Kim YK, Jabbar W, Huang CL.** Conformational changes of pore helix coupled to gating of TRPV5 by protons. *EMBO J* 24: 3224–3234, 2005.
 46. **Yeh BI, Sun TJ, Lee JZ, Chen HH, Huang CL.** Mechanism and molecular determinant for regulation of rabbit transient receptor potential type 5 (TRPV5) channel by extracellular pH. *J Biol Chem* 278: 51044–51052, 2003.